This article was published in Fuel, 159, 854-863, 2015
http://dx.doi.org/10.1016/j.fuel.2015.07.035

Enhancing the low temperature water-gas shift reaction through a hybrid sorption-enhanced membrane reactor for high-purity hydrogen production

M. A. Soria[1], S. Tosti[2], A. Mendes[1], Luis M. Madeira[1*]

[1] *LEPABE – Chemical Engineering Department, Faculty of Engineering - University of Porto, Rua Dr. Roberto Frias, s/n, 4200-465 Porto, Portugal.*

[2] *ENEA – Unità Tecnica Fusione, C.R. ENEA Frascati, Via E. Fermi 45, Frascati (RM) I-00044, Italy.*

[*] Corresponding author. Tel.: +351-22-5081519; Fax: +351-22-5081449; E-mail: mmadeira@fe.up.pt

Abstract

The low temperature water-gas-shift reaction (LT-WGS) has been assessed by means of a hybrid sorption-enhanced membrane reactor (HSEMR) that combines both CO_2 and H_2 removal from the reaction zone. The performance of this reactor has been compared with that obtained by i) a traditional and ii) a sorption-enhanced (only CO_2 is removed) reactor operating in the same operational conditions. Cu/ZnO-Al_2O_3 and K_2CO_3-promoted hydrotalcite materials have been used as a catalyst and CO_2 sorbent, respectively. A self-supported Pd-Ag membrane tube has been used in order to selectively separate the H_2. The CO_2 sorption capacity, in the presence and absence of water vapour, of the potassium-promoted hydrotalcite has been determined by means of breakthrough experiments. The presence of water vapour enhanced the sorption capacity of the hydrotalcite in the experimental conditions used. Concerning the performance of the HSERM, results clearly show that when both CO_2 and H_2 are removed from the reaction zone, the hydrogen production through the reversible LT-WGS reaction is enhanced compared to either a traditional or a sorption-enhanced reactor, allowing overcoming equilibrium limitations and obtain a pure H_2 stream.

Keyword: Water-gas shift, hydrotalcite, CO_2 sorption, membrane reactor, sorption enhanced, hydrogen.

1. Introduction

Hydrogen is an important raw material widely used in the chemical industry (i.e. oil refining and production of bulk chemical such as methanol and ammonia) and as clean energy vector for fuel cells and internal combustion engines [1,2]. Global demand of hydrogen is even growing. Currently, most of the hydrogen produced in the world involves methods such as methane steam reforming (MSR), coal gasification, water electrolysis, biomass gasification and thermochemical process, being MSR the most widely used among them [3,4]. In MSR, the outlet stream contains a large amount of CO as by-product along with hydrogen (H_2/CO ratio >3); the CO content varies between 8 % and 10 % depending of the feedstock composition and conditions used [5]. In order to purify the hydrogen in the MSR reactor effluent and/or tune the CO/H_2 ratio, the syngas stream can be treated in a water-gas shift (WGS, eq. 1) reactor.

$$CO + H_2O = H_2 + CO_2 \qquad \Delta H^0_{298} = -41 \text{ kJ mol}^{-1} \qquad (1)$$

This chemical equilibrium-limited reaction is a mildly exothermic and hence is thermodynamically favoured at low temperatures, although kinetically favoured at high temperatures. For this reason, to obtain high CO conversion, the WGS reaction is industrially carried out in two successive steps at different temperatures, namely: (i) a high-temperature water gas-shift (HT-WGS) reactor operating between 350 ºC and 550 ºC and (ii) a low-temperature water-gas shift (LT-WGS) reactor at 200-300 ºC. The first shift reactor works with iron-chrome oxide catalysts and has an output stream containing 1.5-4.0% CO, while the second reactor operates with copper-zinc oxide catalysts where the CO outlet composition is reduced to about 0.5-1.0% [5,6].

The gas produced from the WGS reaction contains other components (mainly CO, CO_2, H_2O and CH_4) apart from H_2. Remaining steam can be relatively easily removed by water condensation, while CO_x and CH_4 are often removed through processes such as pressure

swing adsorption (PSA) to produce high purity hydrogen [7]. This PSA process generally operates at near ambient temperature (20-40 ºC) using CO_2 microporous physisorbents such as activated carbons and zeolites [8]. With this cyclic PSA, hydrogen with 99.99 % purity is obtained but the H_2 recovery is about 75-90 % only since part of the H_2 recovered is used to regenerate the adsorbent [9]. This means that a considerable amount of H_2 produced in this process is lost.

One alternative to the PSA process to separate H_2 is by removing it from the reaction zone by means of one H_2 perm-selective membrane. In this way, not only is possible to obtain ultra-pure H_2, suitable for fuel cells [5], but also the equilibrium limitation can be circumvented by shifting the WGS reaction to the products side in a single unit. Hydrogen perm-selective membranes have been developed using mainly palladium and its alloys [10-12]. These Pd-based membranes show a very high H_2 selectivity and allow reaching CO conversions close to 100 % in membrane reactors (MR) for the LT-WGS reaction [11,13].

On the other hand, the capture and simultaneous separation of CO_2 from the reaction zone has also been proposed [9,14]. This process, so called sorption enhanced water gas shift, allows to overcome the equilibrium limitation maximizing the H_2 production from the syngas as well. Different oxide materials as CO_2 sorbent, such as calcium oxide, lithium zirconates and lithium silicates, have been extensively studied [15,16]. Nevertheless, these sorbents have a poor CO_2 capacity at low temperatures and for their regeneration temperatures above 700 ºC are required. Furthermore, these materials exhibit a progressive loss of their CO_2 sorption capacity under consecutive cycles of adsorption-desorption. However, hydrotalcite-like (HTs) materials could be an attractive option for CO_2 sorption because of their high sorption capacity at lower temperatures (200-400 ºC), which are compatible with WGS reaction [17-19]. Moreover, HTs present a lower

requirement of energy input for their regeneration, as well as acceptable working capacity after multiple cycles and suitable kinetics of carbon dioxide sorption and desorption [18-20].

A new field of research herein addressed deals with the study of innovative multifunctional reactors by combining the MR concept with the sorption-enhanced one. This has a large number of advantages: (i) the process may be performed in a single unit, which simplifies the overall hydrogen production, (ii) compared to a MR, it allows decreasing the required Pd membrane area, often limitative due to its price, (iii) the reaction may be conducted with a lower H_2O/CO ratio, thereby reducing steam usage and operational costs, (iv) fuel-cell grade (i.e. high-purity) hydrogen can be directly produced, and (v) the process captures CO_2, so that is environmentally friendly and allows eliminating the need for a dedicated CO_2 capture unit.

The aim of this work is to study this new concept in a multifunctional hybrid sorption-enhanced membrane reactor. For this purpose, a self-supported Pd-Ag membrane and a commercial hydrotalcite mixed with a LT-WGS Cu-based catalyst have been used. In practice, and because the sorbent regeneration is necessary when the CO_2 starts breaking through the column, and to ensure a continuous production, the use of two parallel reactors is envisaged; while one of them is producing H_2, the other one is the regeneration stage. Thus, each of these reactors requires repetition of reaction-regeneration cycles along time.

2. Experimental

For the experiments, a commercial K_2CO_3 promoted hydrotalcite supplied by Sasol was used. This material, containing 17 wt. % of K_2CO_3 and Mg/Al mass ratio of 0.5, was labelled as MG30-K.

2.1. Thermogravimetric and differential scanning calorimetry (TG-DSC) analysis.

TG-DSC analysis of fresh MG30-K sample was performed in a thermobalance NETZSCH SSA 449F3 Jupiter. Approximately 20 mg of sample was placed in a platinum basket and heated in N_2 flow (50 ml_N/min) from room temperature up to 900 °C at a heating rate of 10 °C/min. All data analyses were performed using NETZSCH Proteus Thermal Analysis software.

2.2. Breakthrough measurements.

Carbon dioxide breakthrough runs were carried out in a stainless steel tube (120 mm long and with 10 mm o.d.), which was placed into an electric oven (Memmert, Type UNE200), controlled by a programmable temperature controller. 2.8 grams of hydrotalcite framed in both ends by mean of two discs of stainless steel mesh (10-15 µm) were used. In order to minimize pressure drop along the bed, the particle size of the hydrotalcite used in the experiments was between 355-550 µm. Before the experiments, the MG30-Ksample was heated under 100 ml_N/min of N_2 at 300 ºC during 2h (to remove loosely interlayer water, as described below).

Experiments were carried out in the presence as well as in absence of water vapour. Thus, different feeds were used: (i) for dry conditions 10 or 15 vol. % of CO_2 and balance N_2 and (ii) for wet conditions 15 vol. % of CO_2, 5, 15 or 25 vol. % of H_2O and balance N_2. Both CO_2 and N_2 were fed to the process with mass flow controllers (model F201 from Bronkhorst High-Tec) whereas the water vapor was produced in a Controlled Evaporation and Mixing (CEM) system (Bronkhorst High-Tec). In both cases, the total flow rate (dry basis) was kept at 100 ml_N/min. The experiments were carried out at 1, 2 and 3 bar of total pressure.

Evolution of the outlet CO_2 dry composition was monitored by an online infrared based CO_2 analyser (model 4210 from Servomex); the H_2O present in the outlet stream was condensed through a Peltier based cold-trap located at the exit of the sorber and prior to the analyser. With the purpose of determining the dead volume in the system, for correcting the breakthrough time and determining the total CO_2 uptake, blank experiments were performed in the same operational conditions but using only glass beads of the same size to fill the column.

The regeneration capacity of the sorbents was assessed in multiples sorption-desorption cycles. The procedure was as follows: (i) sorption step, performed until the feed concentration (dry basis) was reached at the column outlet and (ii) desorption step, carried out under N_2 flow (100 ml_N/min) until almost no CO_2 was detected in the outlet stream (~30 min). The CO_2 sorption capacity of the hydrotalcite was calculated integrating the area above the breakthrough curve and from the molar flow rate and mass of sorbent. The breakthrough time was defined as the instant at which 5 % of the inlet concentration was reached.

2.3 Sorption enhanced water-gas shift reactor (SER) experiments.

Experiments were carried out in a fixed-bed reactor. This reactor consists in a stainless steel tube with a length of 120 mm and 10 mm o.d., loaded with a commercial Cu/ZnO-Al_2O_3 catalyst (supplied by REB Research & Consulting; Ø = 250 -550 μm), mixed with MG30-K sorbent (Ø = 355 -550 μm) in a catalyst/sorbent weight ratio of 1/12 and framed in both ends by two discs of stainless steel mesh (10-15 μm).

The Cu-based catalyst was firstly reduced at 300 ºC for 2 h under a mixture of 15 vol. % H_2 diluted in N_2 (45 ml_N/min of total flow rate); subsequently, the system was flushed with nitrogen (ca. 50 ml_N/min) during 30 min to remove H_2.

162 The sorption enhanced tests were performed at 3 bar, at 250 and 300 ºC, with a feed of
163 CO (10 vol. %), H_2O (15 vol. %) and N_2 (75 vol. %) and a total flow rate of 100 ml_N/min.
164 The contact time, W_{cat}/Q_{CO}, used was 3.7 x 10^{-4} g_{cat} h ml_N^{-1}.
165 The units that compose the experimental set-up have been described in detail elsewhere
166 [21]. The evolution of the outlet stream composition (i.e. mole fraction of CO and CO_2)
167 was monitored online by means of an infrared CO and CO_2 analyzer (Servomex, model
168 4210, accuracy of the measurement ±1% FS). Gas chromatography was used to detect
169 other products, apart from CO and CO_2.
170 Table 1 summarizes the different operating conditions used for the tests described in this
171 section, aiming comparing the traditional packed-bed reactor with the sorption-enhanced
172 reactor.
173 2.4 Hybrid sorption-enhanced membrane reactor (HSEMR) experimental system.
174 A self-supported Pd-Ag membrane tube was used in order to selectively separate the
175 formed H_2 from the reaction zone. Such a tube was produced by means of cold-rolling
176 and diffusion welding according to a previously described technique [11,22]. An annealed
177 commercial metal foil with 50 µm thickness and 25 wt. % of Ag (from Johnson Matthey)
178 has been used for this purpose. The total length and diameter of the permeator tube were
179 120 and 10 mm respectively, being that the Pd-Ag membrane (50 mm of length) was
180 placed in the middle of the tube.
181 HSEMR experiments were carried out in the same setup and experimental conditions
182 described in section 2.3, except that in this case a catalyst/sorbent mass ratio of 1/5 was
183 used. The amount of sorbent used for HSEMR and SER tests was smaller than for the
184 tests described in section 2.3 because the length of the Pd-Ag membrane is lower than
185 that of the reactor tube used for SER. The operational conditions used in the tests
186 described in this section are compiled in Table 2. Particularly, higher pressures were

employed in the retentate side, but to respect the limited resistance integrity of the used self-supported membrane, total pressure difference across the membrane was not higher than 2. However, because a high sweep gas (nitrogen) flow rate was employed, partial pressure of hydrogen in the permeate side is negligible, allowing this way to increase permeation driving force.

Fig. 1 displays the HSEMR configuration, in which the sorbent along with the catalyst are placed inside the Pd-Ag membrane tube. The feed is introduced by the smaller diameter tube and then goes through the sorbent-catalyst bed; the H_2 that permeates from the reaction zone is swept away by the N_2 through the annular region formed by the concentric Pd-Ag membrane and shell tubes.

Prior to the test, the membrane was activated until the permeate H_2 flow rate was constant. Such activation was performed feeding 60 ml_N/min of pure H_2 at 3.5 bar of pressure and using 300 ml_N/min of N_2 as sweep gas in the permeate side (P = 1 bar).

For both SER and HSEMR tests, carbon monoxide conversion was defined as follows:

$$X_{CO}\,(\%) = \frac{F_{CO}^{in} - F_{CO}^{out}}{F_{CO}^{in}} \text{ x } 100 \qquad (2)$$

where F_{CO}^{in} and F_{CO}^{out} are respectively the molar rate flows of CO at the inlet and outlet of the reactor.

3. Results and discussion

3.1 TG/DTG/DSC analysis

Fig. 2 shows the TG/DSC profile for the as supplied MG30-K hydrotalcite. This sample exhibits a two-step mass loss: (i) around 7 % of the initial mass is lost between room temperature and 300 ºC and (ii) further 6 % from 300 ºC to 900 ºC. The mass loss rate is higher for low temperatures (<200 ºC) and then slightly decreases as the temperature increases.

The DSC profile exhibits three endothermic peaks; at ~90 ºC related to physical desorption of loosely interlayer water, at ~400 ºC attributed to dehydroxylation and carbon dioxide removal and at ~700 ºC which was assigned to K_2CO_3 decomposition [23-27].

According to the information provided by the supplier, the MG30-K hydrotalcite was previously calcined at 250 ºC for 1 h and then heated at 450 ºC for 24 h. This suggests that the decarbonation that is typically observed in K_2CO_3 promoted hydrotalcites [28] already occurred during the previous thermal treatment made by the supplier. Indeed, the mass loss at around 400 ºC was small, indicating that the amount of carbonates present in the as supplied MG30-K is very low. This is confirmed by the short peak observed in the DSC profile at said temperature. Hence, the mass loss observed in our case is probably due to the elimination of carbonate that remains in the sample or from CO_2 present in the atmosphere, which was sorbed and incorporated into the structure during storage.

On the other hand, in order to perform breakthrough and other experiments, the MG30-K was previously heated for 2 h at 300 ºC (as described in section 2.2). In such thermal condition, the loosely interlayer water would be removed according to the results observed in TG. As the carbonates are almost not present in the sample, it was not necessary a thermal pre-treatment at higher temperatures inasmuch as the sample already possess a molecular structure having high affinity for CO_2.

3.2 CO_2 breakthrough measurements

The results obtained during CO_2 (15 vol. %) sorption for the MG30-K at 300 ºC and different total pressures are shown in Fig. 3. The plots display the evolution of the normalized CO_2 molar fraction [$y(t)/y^0$] in the outgoing gas as a function of time. As observed in this figure, for all the pressure assessed, the outlet CO_2 molar fraction (y_{CO_2}) reaches the fed value ($y^0_{CO_2}$) after about 960 s. However, the higher is the CO_2 partial

236 pressure, the higher are both the breakthrough time and the total CO_2 capacity (inset of
237 Fig. 3).
238 On the other hand, the breakthrough time increases when the CO_2 feed composition
239 decreases (15 vs 10 vol. %) at constant pressure as can be seen in Fig. 4. But in this case
240 the total CO_2 capacity diminishes from 0.41 to 0.36 mol/kg. Such increase of the
241 breakthrough time observed is due to the CO_2 flow rate, which decreases, and therefore
242 longer is the time required by the sorbent to begin being saturated with the sorbate. In
243 fact, because the CO_2 isotherm is of the favorable type, the concentration front moves at
244 a higher velocity for increasing CO_2 concentrations [29].

245 3.2.1 Study of sorption-desorption cycles

246 The regeneration and stability of the sorbent is a very important aspect for its application
247 in industrial processes that require successive cycles of sorption-desorption. Fig. 5 shows
248 the variation of the relative CO_2 concentration as a function of the sorption-desorption
249 time for the MG30-K hydrotalcite. In the same figure it is represented the measured CO_2
250 sorption capacity (on the right y-axis) and the cycle number (on the top x-axis). The first
251 cycle represents the CO_2 sorption by the fresh sample while cycles from second to sixth
252 correspond to CO_2 sorption after desorption under pure N_2 flow. It is observed that the
253 CO_2 sorption capacity undergoes a sharp decrease from the first to the second cycle, from
254 0.41 to 0.25 mol/kg, which corresponds to a loss of 40 %. However, from the third cycle
255 on, the CO_2 sorption capacity (0.22 mol/kg) remains almost unchanged with the number
256 of cycles; in this case the CO_2 sorption capacity is 46 % lower than the initial value
257 measured in the first cycle. This suggests that, in dry conditions, only 54 % of the initial
258 CO_2 sorption capacity can be used, while the rest (0.19 mol/kg) remains irreversibly
259 sorbed on the hydrotalcite. A similar behavior has been also reported previously [19,26].
260

261 It is well known that the presence of water vapour improves the CO_2 sorption capacity of
262 hydrotalcites [26,30]. This is a very important aspect for the sorption-enhanced WGS
263 reaction since the feed contains water vapour, which could influence the hydrotalcite
264 sorption capacity of CO_2 produced during the reaction. Therefore, it was assessed the
265 effect of different water vapour compositions on the CO_2 sorption capacity of MG30-K
266 hydrotalcite. Fig. 6 exhibits the CO_2 sorption breakthrough curves in consecutive
267 sorption–desorption cycles over the MG30-K hydrotalcite under wet conditions (15 vol.
268 % of water vapour); for practical reasons only until the third cycle is shown. The second
269 and third cycles correspond to CO_2 sorption after desorption under N_2 flow at 300 ºC and
270 1 bar. Table 3 presents the sorption capacity as a function of the cycle number, for these
271 and other experiments with different H_2O contents in the feed. It is observed that the
272 higher is the quantity of water vapour fed, the higher is CO_2 sorption capacity. However,
273 for the same water composition, it decreases with the number of cycles (but only up to
274 the third), being this effect more significant between the first and second cycle. Hence, a
275 similar trend regarding to sorption-desorption cycles, in dry conditions, was observed.
276 However, in wet conditions, a lower loss of the sorption capacity was observed in the
277 second and third cycle, remaining constant afterwards (data not shown). Comparing the
278 behaviour of the MG30-K in dry and wet conditions (Table 3), it is clear that the presence
279 of water vapour enhances considerably the sorption capacity. This issue and the fact that
280 the sorbent shows a higher reversibility during sorption-desorption cycles is essential for
281 its practical application in the sorption-enhanced WGS process. It should be noted,
282 however, that when an excess of water vapour (25 vol. %) was fed, the sorption capacity
283 was not linearly improved as it was observed for 5 and 15 vol. % (Table 3). It was reported
284 that an excess of water, sorbed on the surface, does not improve the sorption capacity,
285 which was associated with an increase of the diffusion resistance due to shrinkage of the

pore mouths [31]. Moreover, for 25 vol.% of water in the feed, the hydrotalcite sorption capacity in the consecutive cycles did not remain so high as for 5 and 15 vol.% (Table 3). The positive effect on the CO_2 sorption capacity in presence of water vapour is likely due to structural changes of the hydrotalcite-like sorbent. It was suggested that water molecules react with Mg and Al oxide producing hydroxides that react with CO_2 forming its respective bicarbonates [32].

3.3 Sorption enhanced water-gas shift

The CO_2 and CO composition (on a dry basis), as well as the CO conversion obtained during WGS reaction in both traditional fixed-bed and sorption-enhanced reactor, at 250 ºC and 300 ºC and 3 bar, are represented in Fig. 7(A-D). As can be seen in figure 7A (300 ºC), the CO_2 and CO are detected simultaneously in the reactor outlet, meaning that both gases start breaking through the bed at the same time. However, the CO composition attains a steady value (~1 %) at about 2 minutes while in the case of CO_2 it takes around 6 minutes to reach a stable value of ~9.5%. Regarding to the CO conversion, from ca. 2 minutes of reaction it has a constant value (~92 %), which is close to the thermodynamic equilibrium value (~96 %, calculated based on feed conditions).

For the test carried out at 250 ºC and 3 bar (Fig. 7B), the CO and the CO_2 also break through the bed at the same time. The CO composition reaches a maximum in the first two minutes, then steadily decreases until it stabilizes after 30 minutes of reaction while the CO_2 composition strongly increases in the 5 initial minutes and then tends to stabilize reaching a plateau. With regard to the CO conversion, it decreases in the first two minutes, and then stabilizes according to the variation of CO composition. The CO and CO_2 composition reach constant values of 1.8 and 8.6 vol. %, respectively. Such a steady-state composition represents a CO conversion close to 83 % (under such conditions equilibrium conversion is 98 %). While thermodynamic equilibrium conversion is higher

311 in Fig. 7B (250 ºC) than in Fig. 7A (300 ºC), which is a consequence of the exothermic
312 nature of the WGS reaction, the opposite occurs for the fixed bed reactor performance,
313 due to kinetic reasons.

314 In order to verify if the MG30-K hydrotalcite is catalytically active towards the WGS
315 reaction in the herein used working conditions, a test employing only the sorbent has been
316 performed. For the test carried out over the MG30-K hydrotalcite at 300 ºC and 3 bar, the
317 CO composition became stable after 20 minutes (data not shown) reaching a value of 11.2
318 vol. % on a dry basis, while the CO_2, which is absent in the feed, presents a breakthrough
319 time close to 5 minutes and a composition of 0.4 vol. % after 30 minutes of reaction. This
320 evidences that the WGS reaction takes place at 300 ºC without the Cu/ZnO-Al_2O_3
321 catalyst, but the values of CO conversion obtained with the hydrotalcite are very low
322 (about 4.5%). Contrarily to what was observed at 300 ºC, at 250 ºC the MG30-K
323 hydrotalcite does not catalyses the WGS reaction (data not shown). Maroño *et. al*. [33]
324 have also observed that the hydrotalcite is catalytically active for the WGS reaction, but
325 for a range of temperatures between 300 ºC and 400 ºC and 14 bar of pressure. In that
326 case a higher CO conversion was observed; however, the sorbent strongly loses its
327 catalytic activity when submitted to reaction-regeneration cycles. In our case, since the
328 hydrotalcite shows a low activity in the conditions assessed, its behavior under reaction-
329 regeneration cycles was not studied into further detail.

330 Fig. 7C illustrates the effect of carrying out the CO_2 sorption and the WGS reaction
331 simultaneously, in this case using MG30-K and Cu/ZnO-Al_2O_3 as sorbent and catalyst,
332 respectively, in a mixed bed. The sorption-enhanced concept is clearly shown by
333 comparing Figures 7A and 7C. In fact, it is possible to observe that when a mixture of
334 sorbent and catalyst is used, the CO_2 breakthrough time is delayed about 2 minutes (Fig.
335 7C) as compared to the time taken for the test carried out in the same operational

336 conditions but only with the catalyst (Fig.7A). This suggests that, in the pre-breakthrough
337 zone, while the CO_2 is selectively removed from the gas phase by means of the sorbent,
338 the reaction is being shifted to produce more H_2. This is corroborated by the fact that in
339 the pre-breakthrough zone no CO was detected in the outgoing gas, and therefore the CO
340 conversion is complete, indicating that the equilibrium limit was overcome. When the
341 hydrotalcite reaches its CO_2 sorption capacity and gets saturated, the compositions of CO
342 and CO_2 are very similar to the values measured for the test with catalyst only (cf.
343 Fig.7A); in fact, the CO conversion in such zone is slightly higher. This is probably due
344 to the fact that, as previously mentioned, the hydrotalcite showed a certain catalytic
345 activity in these conditions (300 ºC and 3 bar).

346 Fig.7D presents the history of y_{CO_2} and y_{CO} values at the exit stream during the WGS
347 reaction, which was carried out at 250 ºC and 3 bar over a mixed bed containing the
348 Cu/ZnO-Al_2O_3 catalyst and the MG30-K sorbent. It is observed the CO_2 breakthrough at
349 about 2 minutes, while the CO is detected since the beginning; the CO_2 and CO
350 compositions reach a steady- state after about 30 minutes. In the pre-breakthrough zone
351 the CO composition is lower than for the test carried out only with catalyst. This suggests
352 that the presence of the MG30-K hydrotalcite as a CO_2 sorbent shifts the WGS reaction,
353 but in this case does not overcame the thermodynamic equilibrium. As above-mentioned,
354 although the WGS reaction is thermodynamically favored at lower temperatures, the
355 opposite occurs in term of the reaction rate and thus the reaction is kinetically controlled
356 [21].

357 3.4 Hybrid sorption-enhanced membrane reactor system

358 In order to study the effect of the permselective membrane on the CO conversion, apart
359 from the hydrotalcite and catalyst mixture, a self-supported Pd-Ag membrane (thickness
360 of 50 μm) was employed in a hybrid sorption-enhanced membrane reactor (HSEMR).

361 In previous works, it was reported that the method used (diffusion welding technique)
362 allows preparing reproducible, long term stable and nearly infinite permselective Pd-Ag
363 membranes towards H_2 [11,34-36], thus meaning that the hydrogen recovered would be
364 a COx-free stream. Permeability of such membranes towards hydrogen under different
365 conditions has also been reported in such works.

366 Figure 8 shows the evolution of the CO and CO_2 concentration as well as the CO
367 conversion as a function of time for the test performed in a SER at 300 ºC and 3 bar of
368 total pressure (Fig. 8A), and the tests performed in a HSEMR at 300 ºC and 3.0, 4.0 and
369 5.5 bar of total pressure in the retentate side (Figs. 8B, 8C and 8D, respectively).

370 In comparison with the test carried out over Cu/ZnO-Al_2O_3 only – TR (Fig.7A), it is
371 evident that, for the test performed at 300 ºC and 3 bar in the HSEMR (Fig. 8B), in the
372 pre-breakthrough zone, neither CO nor CO_2 were observed in the reactor outlet (within
373 the detection limits), indicating that a full CO conversion was achieved and hence two
374 high-purity hydrogen stream were produced. This aspect is very noticeable when it is
375 envisaged to couple this technology to a system where the presence of CO could be
376 prejudicial like a fuel cell.

377 As in the test carried out with catalyst and sorbent – SER (cf. Fig. 8A), in the HSEMR is
378 also observed that the CO concentration reaches a steady-state value when CO_2
379 concentrations stabilizes, i.e., when the hydrotalcite becomes saturated. But in this case,
380 due to the presence of the Pd-Ag membrane, at steady-state the CO conversion is slightly
381 higher and pretty close to the equilibrium one. As was reported in a previous work [35],
382 both the CO and the CO_2 affect the H_2 permeation through the membrane, which would
383 explain why in the post-breakthrough zone the presence of the Pd-Ag membrane seems
384 to not greatly improve the reaction (H_2 recovery of 18 %). But in a system with two
385 parallel reactors alternating between reaction/sorption and regeneration, the interest is

386 centered in the pre-breakthrough zone in order to ensure a continuous high-purity H_2
387 production from the retentate side. Such hydrogen can be added to that coming from the
388 permeate side, providing 100% H_2 recovery. In such zone all the CO_2 is sorbed by the
389 hydrotalcite and the CO is not produced (the equilibrium is completely shifted), which is
390 favorable for the Pd-Ag membrane avoiding thus its deterioration.

391 Fig. 8C and 8D displays the evolution of CO and CO_2 concentration for the tests carried
392 out in a HSEMR at 300 ºC at 4 and 5.5 bar of total pressure in the retentate side,
393 respectively. In both cases, the CO_2 breakthrough time is higher than that of the test
394 performed in the HSEMR at 300 ºC but at 3 bar of total pressure (Fig. 8B), which is likely
395 due to an effect of the pressure which increases the CO_2 breakthrough time, as shown in
396 the breakthrough experiments (cf. section 3.2). One can consider that in the tests
397 performed at 3, 4 and 5.5 bar (Figures 8B, 8C and 8D) the retentate composition in the
398 pre-breakthrough zone is the same because the CO conversion is complete.

399 A similar shape of the CO and CO_2 composition profiles was observed at 4 and 5.5 bar
400 with respect to those observed when the test was performed at 300 ºC and 3 bar (Fig.8B)
401 except that in this case the values of CO conversion at steady-state are higher, reaching
402 (at 4 bar) or even overcoming (at 5.5 bar) the equilibrium. This can be related to the higher
403 driving force for H_2 permeation. In fact, the H_2 recovery was 23 % and 37 % for the tests
404 performed at 4 bar and 5.5 bar, respectively.

405 The performance of the sorption enhanced reactor (3 bar) and hybrid sorption-enhanced
406 membrane reactor (3 or 5.5 bar in the retentate side) was also studied at 250 ºC (Fig. 9).
407 In Figure 9B and 9C, it is observed that the CO_2 produced during the WGS reaction is
408 completely sorbed until it stars to break through the bed (pre-breakthrough zone); then its
409 exit concentration continuously increases with the time on stream till steady state is
410 reached. However, in the test performed at 3 bar, the CO is already detected at the

411 beginning of the reaction while at 5.5 bar both CO and CO_2 start breaking through the
412 bed later, and at the same time. At 3 bar as 5.5 bar the CO composition steadily raises
413 after breaking through the bed; in accordance with this, the CO conversion decreases
414 along the reaction time. It is worth highlighting that the CO outgoing composition
415 measured in the pre-breakthrough zone is lower than that measured for the sorption
416 enhanced reactor (Figure 9A). This means that the CO conversion in the HSEMR is higher
417 than that in the SER, reaching the equilibrium conversion (100 %) for the tests carried
418 out at 5.5 bar at a temperature as low as 250 ºC. In this regard, it is possible to conclude
419 that the coexistence of both the membrane (for H_2 separation) and the sorbent (for CO_2
420 adsorption) act simultaneously, being thus possible to further reduce the CO content in
421 the exit stream. The H_2 recovery was 12 % and 25 % for the tests performed at 3 bar and
422 5.5 bar, respectively.
423
424 3.5 Perspective of implementation of the hybrid sorption-enhanced membrane reactor
425 As mentioned above, the HSEMR simultaneously carries out the WGS reaction while
426 removing hydrogen and carbon dioxide from the reaction zone, respectively (Fig. 10).
427 The continuous use of such configuration would require the cyclic operation of two
428 parallel reactors (if regeneration is not longer than the production stage), producing (Fig.
429 10a)) and regenerating (Fig. 10b)) out of phase. Since the goal is to shift the
430 thermodynamic equilibrium of WGS during reaction mode by retaining CO_2 in the
431 sorbent, once the sorbent gets saturated and CO_2 starts breaking through the column the
432 reaction is ended (Fig. 10 (a)) and the regeneration stage is initiated (Fig. 10 (b)). The
433 main requirement is that operating conditions in both Reaction and Regenerations stages,
434 namely in terms of temperature, are compatible for the WGS catalyst, CO_2 sorbent and
435 H_2-selective membrane. While at lab scale N_2 was used as sweep (in the membrane side)

436 and purge (for sorbent regeneration) gas, at industrial level the use of steam is preferable,
437 being also easier to separate using a simple water condenser.
438
439 **4. Conclusions.**
440 Results show that the presence of water vapour improves the CO_2 sorption capacity of the
441 MG30-K hydrotalcite during dynamic CO_2 sorption experiments. When such material is
442 submitted to CO_2 sorption-desorption cycles its capacity decreases, but not significantly
443 in the presence of water vapour, and stabilizes after a few cycles. This suggests that this
444 kind of material could be used as CO_2 sorbent, under the operational conditions analyzed,
445 namely in a cyclic sorption-enhanced WGS reactor.
446 The use of the SER packed with MG30-K hydrotalcite along with a Cu/ZnO-Al_2O_3
447 catalyst allowed that the CO conversion, in the pre-breakthrough zone, increases
448 regarding a traditional reactor; such reactor configuration also allows overcoming the
449 equilibrium conversion based on feed conditions, before CO_2 breaks through the column.
450 Finally, when a multifunctional sorption-enhanced membrane reactor is used at 250 ºC
451 and 3 bar, the CO conversion increases even more. In this regard, it is possible to conclude
452 that the coexistence of both the membrane (for H_2 separation) and the sorbent (for CO_2
453 sorption) act simultaneously. However, at higher pressure (5.5 bar) or higher temperature
454 (300 ºC), in the pre-breakthrough zone complete CO conversion is reached, allowing to
455 obtain two hydrogen streams feasible to be fed to a fuel cell (with 100% H_2 recovery).
456 This suggests that combining CO_2 and H_2 removal in a single unit could be beneficial for
457 the high-purity H_2 production. Moreover, in the pre-breakthrough zone, the CO_2 is sorbed
458 by the hydrotalcite and the CO is not produced (the equilibrium is completely shifted),
459 which is favorable for the Pd-Ag membrane since CO_2 and mainly CO in gas phase can
460 poison the membrane, affecting the H_2 permeability.

5. Acknowledgments

This work was supported by project PTDC/EQU/ERQ/098730/2008 - FCOMP-01-0124-FEDER-010380, financed by the European Fund for Regional Development (ERDF) through COMPETE – Programa Operacional Factores de Competitividade – and by national funds through Fundação para a Ciência e a Tecnologia (FCT).

M.A. Soria is grateful to the FCT for his postdoctoral grant (SFRH/BPD/88444/2012), with financing from the European Social Fund (ESF) and the Human Potential Operational Programme (POPH).

6. References

[1] Peña MA, Gómez JP, Fierro JLG. New catalytic routes for syngas and hydrogen production. Appl Catal A: Gen 1996;144:7-57.

[2] Garcia La, French R, Czernik S, Chornet E. Catalytic steam reforming of bio-oils for the production of hydrogen: effects of catalyst composition. Appl Catal A: Gen 2000;201:225-39.

[3] Abbas HF, Wan Daud WMA. Hydrogen production by methane decomposition: A review. Int J Hydrogen Energy 2010;35:1160-90.

[4] Chesnokov VV, Chichkan AS. Production of hydrogen by methane catalytic decomposition over Ni–Cu–Fe/Al2O3 catalyst. Int J Hydrogen Energy 2009;34:2979-85.

[5] Choudhary TV, Goodman DW. CO-free fuel processing for fuel cell applications. Catal Today 2002;77:65-78.

[6] Mendes D, Mendes A, Madeira LM, Iulianelli A, Sousa JM, Basile A. The water-gas shift reaction: from conventional catalytic systems to Pd-based membrane reactors—a review. Asia-Pacific Journal of Chemical Engineering 2010;5:111-37.

[7] Yang S-I, Choi D-Y, Jang S-C, Kim S-H, Choi D-K. Hydrogen separation by multi-bed pressure swing adsorption of synthesis gas. Adsorption 2008;14:583-90.

[8] Lee KB, Verdooren A, Caram HS, Sircar S. Chemisorption of carbon dioxide on potassium-carbonate-promoted hydrotalcite. Journal of Colloid and Interface Science 2007;308:30-39.

[9] Jang HM, Lee KB, Caram HS, Sircar S. High-purity hydrogen production through sorption enhanced water gas shift reaction using K2CO3-promoted hydrotalcite. Chem Eng Sci 2012;73:431-38.

[10] Liguori S, Pinacci P, Seelam PK, Keiski R, Drago F, Calabrò V et al. Performance of a Pd/PSS membrane reactor to produce high purity hydrogen via WGS reaction. Catalysis Today 2012;193:87-94.

[11] Mendes D, Chibante V, Zheng J-M, Tosti S, Borgognoni F, Mendes A et al. Enhancing the production of hydrogen via water–gas shift reaction using Pd-based membrane reactors. International Journal of Hydrogen Energy 2010;35:12596-608.

[12] García-García FR, Soria MA, Mateos-Pedrero C, Guerrero-Ruiz A, Rodríguez-Ramos I, Li K. Dry reforming of methane using Pd-based membrane reactors fabricated from different substrates. Journal of Membrane Science 2013;435:218-25.

[13] Mendes D, Sá S, Tosti S, Sousa JM, Madeira LM, Mendes A. Experimental and modeling studies on the low-temperature water-gas shift reaction in a dense Pd–Ag packed-bed membrane reactor. Chemical Engineering Science 2011;66:2356-67.

[14] van Dijk HAJ, Walspurger S, Cobden PD, van den Brink RW, de Vos FG. Testing of hydrotalcite-based sorbents for CO2 and H2S capture for use in sorption enhanced water gas shift. International Journal of Greenhouse Gas Control 2011;5:505-11.

[15] Martavaltzi CS, Lemonidou AA. Development of new CaO based sorbent materials for CO2 removal at high temperature. Microporous and Mesoporous Materials 2008;110:119-27.

[16] Seggiani M, Puccini M, Vitolo S. High-temperature and low concentration CO2 sorption on Li4SiO4 based sorbents: Study of the used silica and doping method effects. International Journal of Greenhouse Gas Control 2011;5:741-48.

[17] Moreira RFPM, Soares JL, Casarin GL, Rodrigues AE. Adsorption of CO2 on Hydrotalcite‐like Compounds in a Fixed Bed. Separation Science and Technology 2006;41:341-57.

[18] Lee KB, Beaver MG, Caram HS, Sircar S. Reversible chemisorption of carbon dioxide: simultaneous production of fuel-cell grade H2 and compressed CO2 from synthesis gas. Adsorption 2007;13:385-97.

[19] Miguel CV, Trujillano R, Rives V, Vicente MA, Ferreira AFP, Rodrigues AE et al. High temperature CO2 sorption with gallium-substituted and promoted hydrotalcites. Sep Purif Technol 2014;127:202-11.

[20] Martunus, Othman MR, Fernando WJN. Elevated temperature carbon dioxide capture via reinforced metal hydrotalcite. Microporous and Mesoporous Materials 2011;138:110-17.

[21] Soria MA, Pérez P, Carabineiro SAC, Maldonado-Hódar FJ, Mendes A, Madeira LM. Effect of the preparation method on the catalytic activity and stability of Au/Fe2O3 catalysts in the low-temperature water–gas shift reaction. Applied Catalysis A: General 2014;470:45-55.
[22] Tosti S, Bettinali L. Diffusion bonding of pd-ag rolled membranes. Journal of Materials Science 2004;39:3041-46.
[23] Long Q, Xia Y, Liao S, Li Y, Wu W, Huang Y. Facile synthesis of hydrotalcite and its thermal decomposition kinetics mechanism study with masterplots method. Thermochimica Acta 2014;579:50-55.
[24] Yang W, Kim Y, Liu PKT, Sahimi M, Tsotsis TT. A study by in situ techniques of the thermal evolution of the structure of a Mg–Al–CO3 layered double hydroxide. Chemical Engineering Science 2002;57:2945-53.
[25] Li X, Zhu J, Liu Q, Wu B. The removal of naphthenic acids from dewaxed VGO via esterification catalyzed by Mg–Al hydrotalcite. Fuel Processing Technology 2013;111:68-77.
[26] Martunus, Helwani Z, Wiheeb AD, Kim J, Othman MR. Improved carbon dioxide capture using metal reinforced hydrotalcite under wet conditions. International Journal of Greenhouse Gas Control 2012;7:127-36.
[27] Walspurger S, Boels L, Cobden PD, Elzinga GD, Haije WG, van den Brink RW. The Crucial Role of the K+–Aluminium Oxide Interaction in K+-Promoted Alumina- and Hydrotalcite-Based Materials for CO2 Sorption at High Temperatures. ChemSusChem 2008;1:643-50.
[28] Das J, Das D, Parida KM. Preparation and characterization of Mg–Al hydrotalcite-like compounds containing cerium. Journal of Colloid and Interface Science 2006;301:569-74.
[29] Ruthven DM. Principles of Adsorption and Adsorption Processes. John Wiley & Sons, New York, US (1984).
[30] Halabi MH, de Croon MHJM, van der Schaaf J, Cobden PD, Schouten JC. High capacity potassium-promoted hydrotalcite for CO2 capture in H2 production. International Journal of Hydrogen Energy 2012;37:4516-25.
[31] Ficicilar B, Dogu T. Breakthrough analysis for CO2 removal by activated hydrotalcite and soda ash. Catalysis Today 2006;115:274-78.
[32] Ram Reddy MK, Xu ZP, Diniz da Costa JC. Influence of Water on High-Temperature CO2 Capture Using Layered Double Hydroxide Derivatives. Ind Eng Chem Res 2008;47:2630-35.
[33] Maroño M, Torreiro Y, Cillero D, Sánchez JM. Experimental studies of CO2 capture by a hybrid catalyst/adsorbent system applicable to IGCC processes. Applied Thermal Engineering.
[34] Tosti S, Basile A, Bettinali L, Borgognoni F, Gallucci F, Rizzello C. Design and process study of Pd membrane reactors. Int J Hydrogen Energy 2008;33:5098-105.
[35] Miguel CV, Mendes A, Tosti S, Madeira LM. Effect of CO and CO2 on H2 permeation through finger-like Pd–Ag membranes. Int J Hydrogen Energy 2012;37:12680-87.
[36] Tosti S, Basile A, Bettinali L, Borgognoni F, Chiaravalloti F, Gallucci F, Long-term tests of Pd–Ag thin wall permeator tube, Journal of Membrane Science, 2006; 284; 393–397.

570

571

572

573 **Tables**

574

575

576 Table 1. Operational conditions used in tests described in section 2.3 to compare
577 traditional reactor (TR) vs. sorption-enhanced reactor (SER).
578

	TR	SER
Weight of catalyst ($Cu/ZnO-Al_2O_3$) [g]	0.22	0.22
Weight of sorbent (MG30-K)[g]	-	2.6
Catalyst/Sorbent weight ratio	-	1/12
W_{cat}/Q_{CO} [g h ml_N^{-1}]	3.7 x 10^{-4}	3.7 x 10^{-4}
Feed composition $CO/H_2O/N_2$ [vol. %]	10/15/75	10/15/75
T [ºC]	250 , 300	250, 300
$P_{T,feed}$ [bar]	3	3

579

580

Table 2. Operational conditions used in tests described in section 2.4 to compare. sorption-enhanced reactor (SER) vs. hybrid sorption-enhanced membrane reactor (HSEMR).

	SER	HSEMR
Weight of catalyst [g]	0.22	0.22
Weight of sorbent [g]	1.2	1.2
Catalyst/Sorbent weight ratio	1/5	1/5
W_{cat}/Q_{CO} [g h ml_N^{-1}]	3.7 x 10^{-4}	3.7 x 10^{-4}
Feed composition $CO/H_2O/N_2$ [vol. %]	10/15/75	10/15/75
T [ºC]	250, 300	250 , 300
$P_{T,\text{feed}}$ [bar]	3	3, 4 and 5.5
$\Delta P = P_{T,\text{feed}} - P_{T,\text{sweep gas}}$	-	~2*

* Total pressure difference across the membrane was not higher than 2 bar to respect the limited resistance integrity of the used self-supported membrane; the sweep was always nitrogen.

Table 3. CO_2 sorption capacity in dry and wet conditions (mol/kg).

% vol. H_2O	1st cycle	2nd cycle	3rd cycle
0	0.41	0.25	0.22
5	0.48	0.42	0.39
15	0.60	0.53	0.51
25	0.65	0.51	0.48

In all cases: 15 vol. % of CO_2 (balanced with N_2); P_T=1 bar;
From 3rd to the 6th cycle, the sorption capacity remains constant (data not shown).

Figures

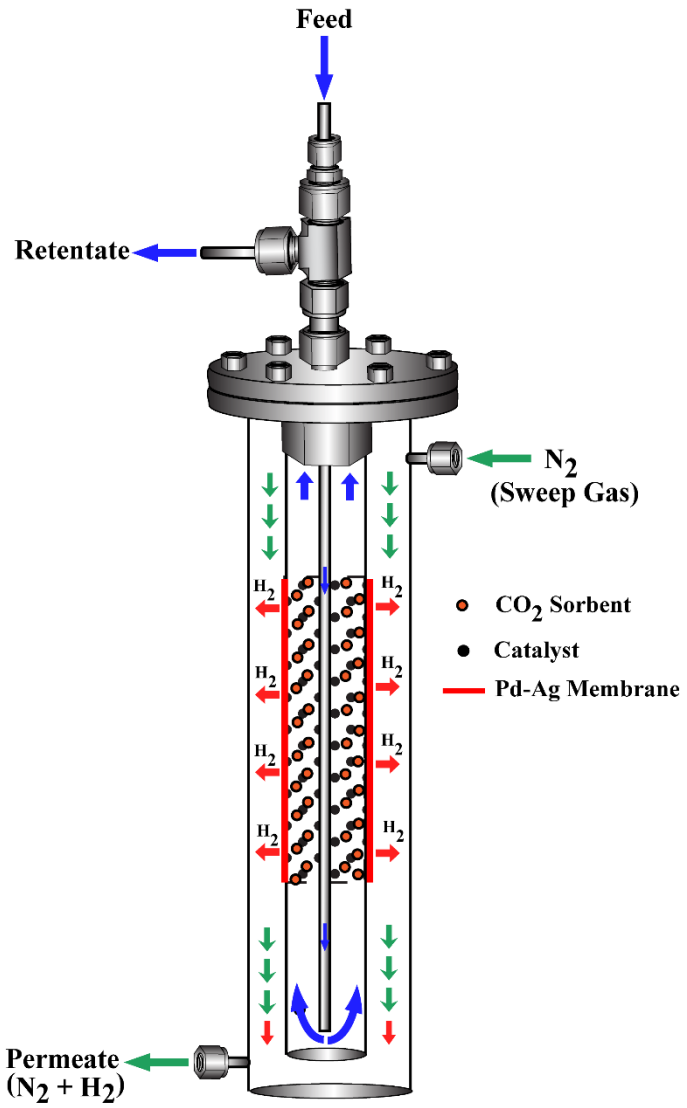

Fig.1. Scheme of the hybrid sorbent-membrane reactor.

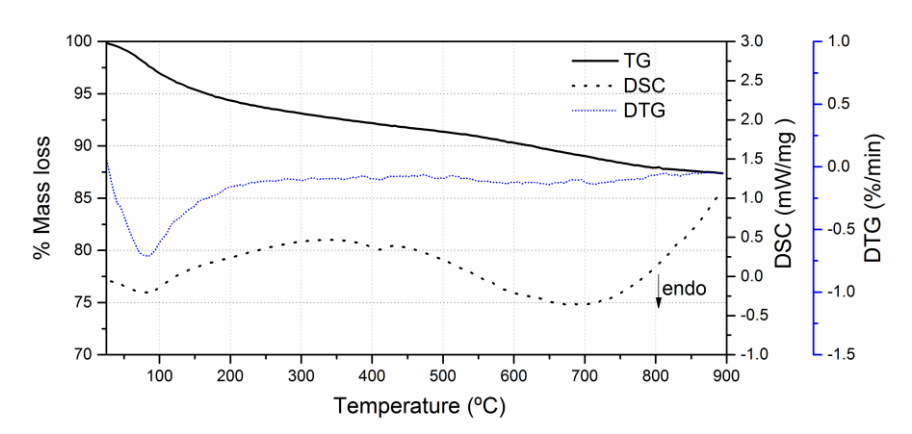

Fig.2. TG/DTG/DSC profiles for the MG30-K promoted hydrotalcite.

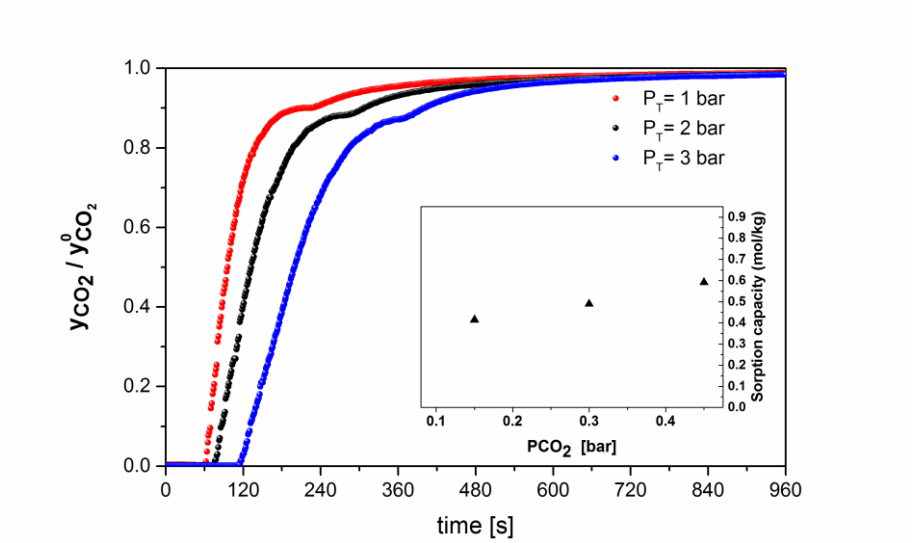

Fig. 3. Experimental breakthrough curves obtained with the MG30-K hydrotalcite at different total pressures (P_T; (•) 1 bar, (•) 2 bar and (•) 3 bar). T = 300 ºC, feed composition =15 vol.% of CO_2 and balance N_2, total flow rate = 100 ml_N/min .

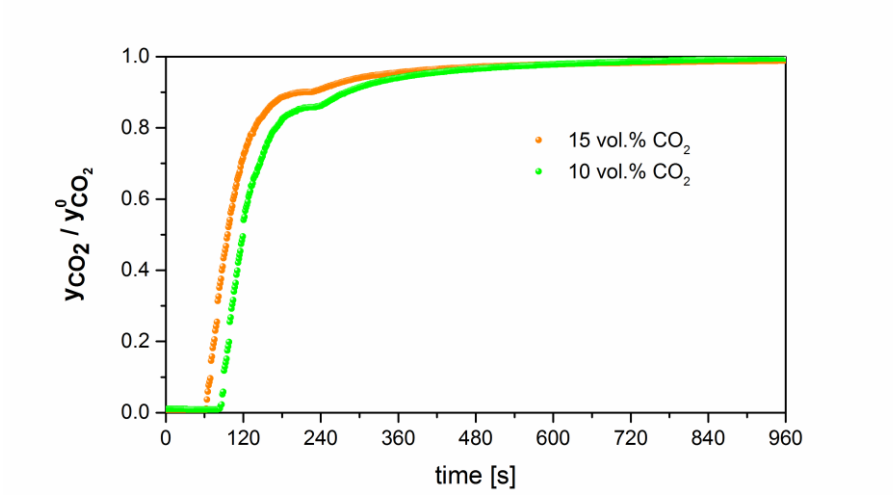

Fig 4. Experimental breakthrough curves obtained with the MG30-K hydrotalcite at different CO_2 feed compositions (•) 15 vol.% of CO_2 in N_2 and (•) 10 vol.% of CO_2 in N_2. T = 300 ºC, P_T= 1 bar, total flow rate = 100 ml_N/min.

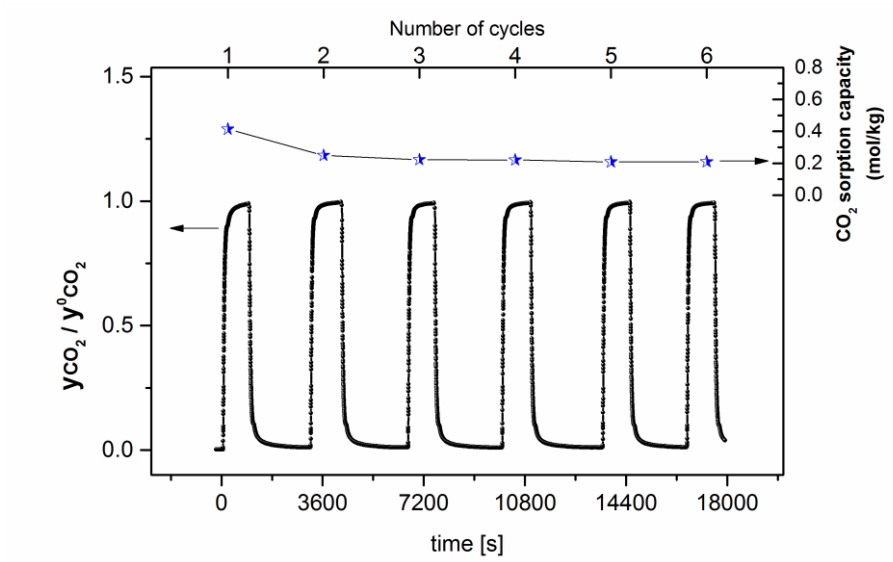

Fig.5. Regeneration behavior in dry conditions; variation of the relative CO_2 concentration and sorption capacity as a function of the sorption time and cycles number of the MG30-K hydrotalcite. Sorption conditions: P_T= 1 bar, T=300 ºC, total flow rate = 100 ml_N/min and feed composition= 15 vol. % of CO_2 in N_2. Desorption conditions: P_T= 1 bar, T= 300 ºC and 100 ml_N/min of N_2.

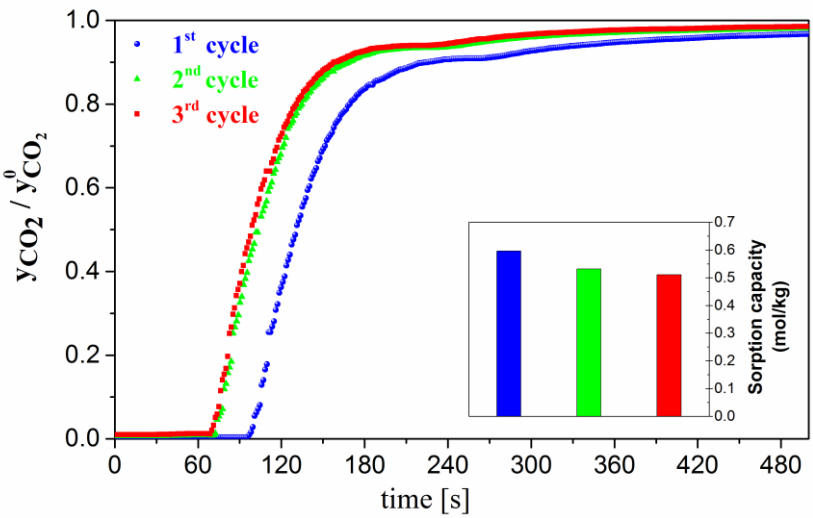

Fig. 6. Breakthrough curves in three consecutive sorption-desorption cycles and corresponding sorption capacities (inset) in presence of water vapour. Sorption conditions: T = 300 ºC, P_T = 1 bar, 15 vol. % of CO_2 and 15 vol. % of H_2O balanced with N_2. Desorption conditions: T = 300 ºC, P_T = 1 bar and 100 ml_N/min of N_2.

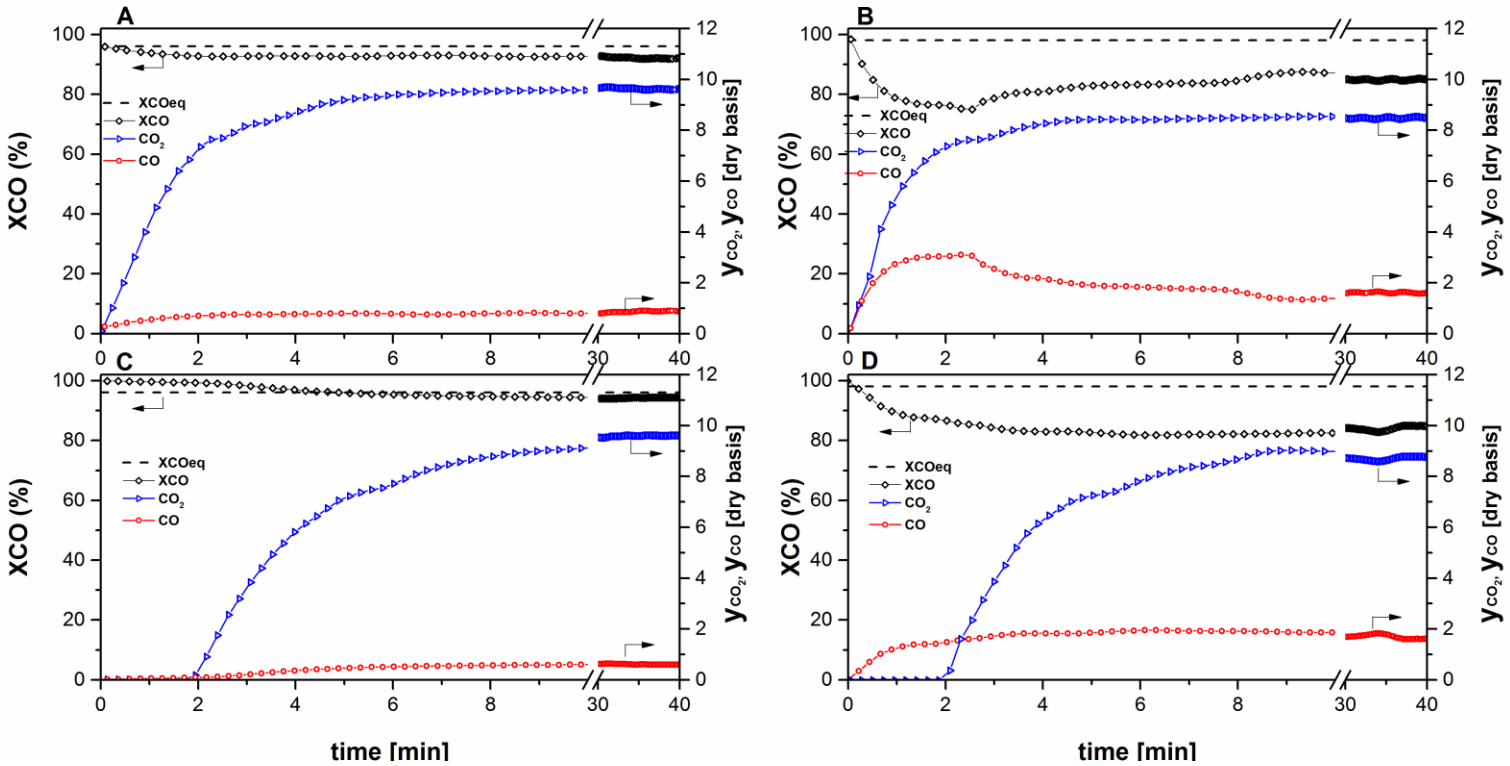

Fig. 7. CO conversion and CO and CO_2 composition (vol. %) history during WGS reaction in a traditional reactor at **A**) 300 ºC and **B**) 250 ºC and in a sorption-enhanced reactor at **C)** 300 ºC and **D**) 250 ºC. See Table 1 for additional operating conditions.

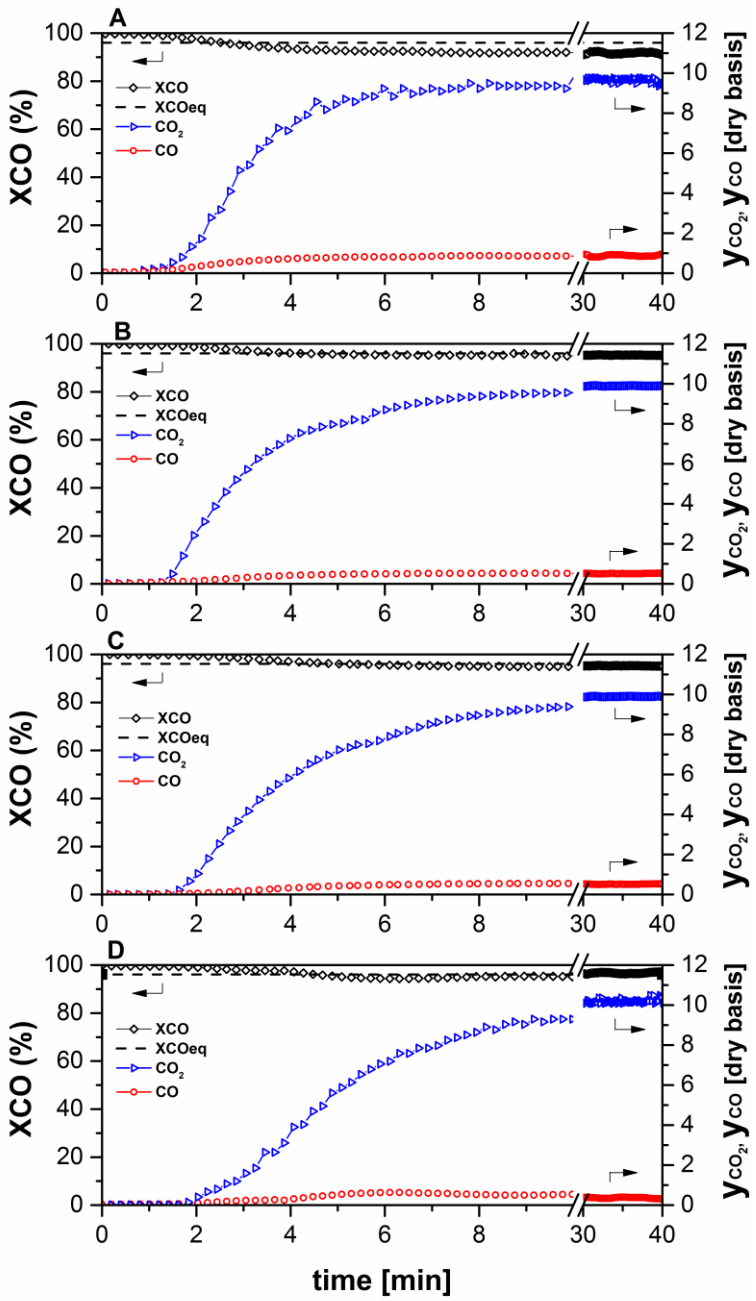

Fig. 8. CO conversion and CO and CO_2 composition (vol. %) history during WGS reaction in a sorption-enhanced reactor at **A**) 300 ºC and 3 bar and in a hybrid sorbent-membrane reactor at **B**) 300 ºC and 3 bar, **C)** 300 ºC and 4 bar and **D**) 300 ºC and 5.5 bar. See Table 2 for additional operating conditions.

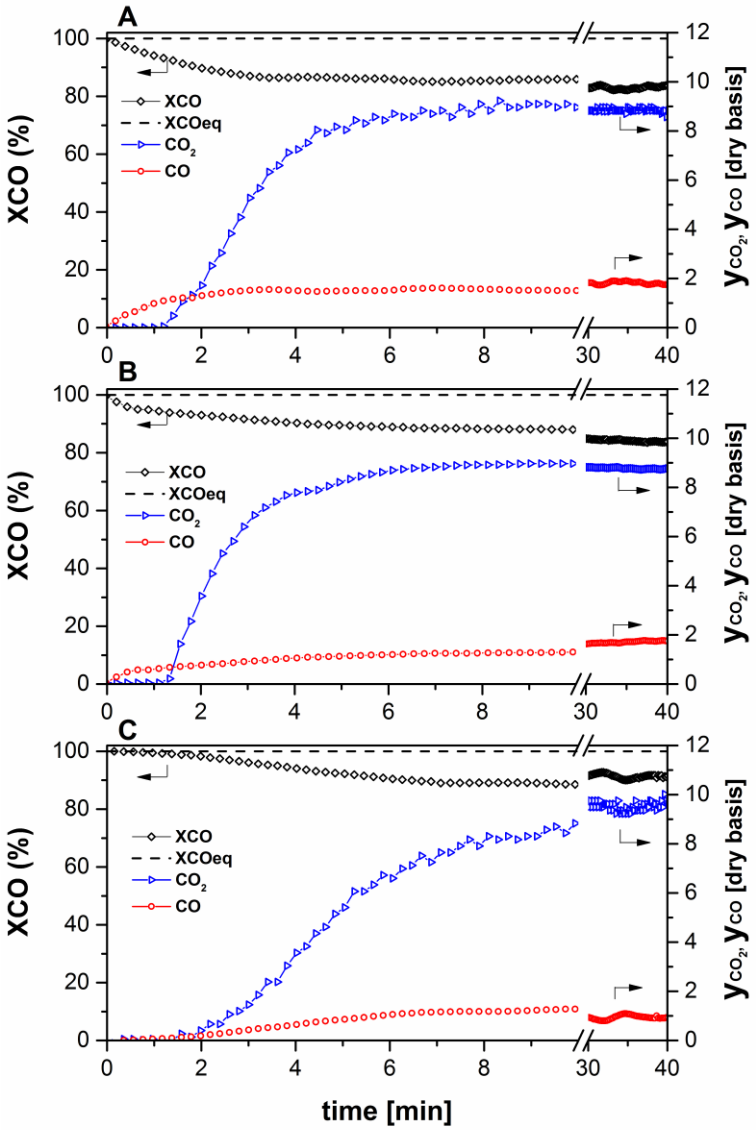

641

642 **Fig. 9.** CO conversion and CO and CO_2 composition (vol. %) history during WGS reaction in a sorption-
643 enhanced reactor at **A**) 250 ºC and 3 bar and in a hybrid sorbent-membrane reactor at **B**) 250 ºC and 3 bar
644 and **C)** 250 ºC and 5.5 bar. See Table 2 for additional operating conditions.

645

646

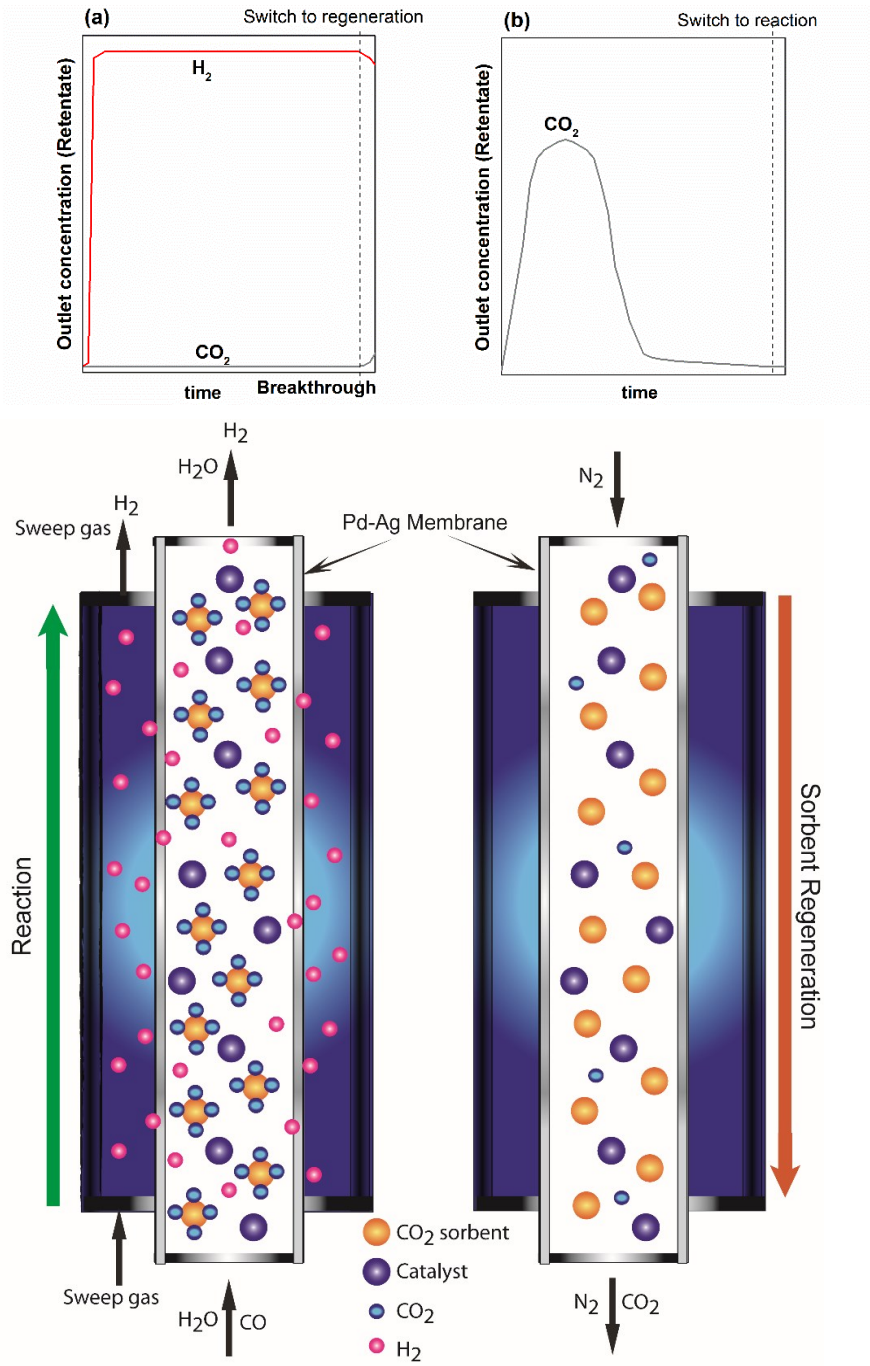

Fig. 10 - Schematic view of the conceived HSEMR based on 2 parallel reactors configuration for continuous operation and corresponding outlet concentrations histories in the retentate stream during (a) reaction and (b) regeneration stages.